REPORT DOCUMENTATION PAGE

Form Approved
OMB No. 0704-0188

1. REPORT DATE *(DD-MM-YYYY)*	**2. REPORT TYPE**	**3. DATES COVERED** *(From - To)*
28-08-2007	Journal Article	

4. TITLE AND SUBTITLE

ExB Measurements of a 200 W Xenon Hall Thruster (Preprint)

5a. CONTRACT NUMBER

5b. GRANT NUMBER

5c. PROGRAM ELEMENT NUMBER

6. AUTHOR(S)
Jared M. Ekholm & William A. Hargus, Jr. (AFRL/PRSS)

5d. PROJECT NUMBER

5e. TASK NUMBER
33SP0706

5f. WORK UNIT NUMBER

7. PERFORMING ORGANIZATION NAME(S) AND ADDRESS(ES)

Air Force Research Laboratory (AFMC)
AFRL/PRSS
1 Ara Drive
Edwards AFB CA 93524-7013

8. PERFORMING ORGANIZATION REPORT NUMBER

AFRL-PR-ED-JA-2007-402

9. SPONSORING / MONITORING AGENCY NAME(S) AND ADDRESS(ES)

Air Force Research Laboratory (AFMC)
AFRL/PRS
5 Pollux Drive
Edwards AFB CA 93524-7048

10. SPONSOR/MONITOR'S ACRONYM(S)

11. SPONSOR/MONITOR'S NUMBER(S)
AFRL-PR-ED-JA-2007-402

12. DISTRIBUTION / AVAILABILITY STATEMENT

Approved for public release; distribution unlimited (PA #07348A).

13. SUPPLEMENTARY NOTES
Submitted for publication in the Journal of Propulsion and Power.

14. ABSTRACT

Angularly resolved ion species fractions of Xe^{+1}, Xe^{+2}, and Xe^{+3} in a low power xenon Hall thruster Busek BHT-200 plume were measured using an ExB probe under a variety of thruster operating conditions and background pressures. The thruster was operated at several operating conditions by varying the anode potential of the thruster from 200 V to 325 V in 25 V increments. Measurements of the ion species fractions were made ±90° from thruster centerline 60 cm downstream of the exit plane. At reduced discharge voltages, the species fractions of multiply-charged xenon ions were lower, while at increased discharge voltages, Xe^{+2} and Xe^{+3} showed an increase in their respective ion species fractions. At angles greater than ±35°, a low energy peak was observed suggesting additional collisions in the far-field produce a low energy ion population. Finally, measurements were directed toward characterizing chamber backpressure effects on the plume species fractions at oblique angles between 35-90°. In the presence of additional background neutrals, production of mutiply-charged ions increased throughout the plume as a result of increased collisions and scattering.

15. SUBJECT TERMS

16. SECURITY CLASSIFICATION OF:			**17. LIMITATION OF ABSTRACT**	**18. NUMBER OF PAGES**	**19a. NAME OF RESPONSIBLE PERSON**
					Dr. William A. Hargus, Jr.
a. REPORT	**b. ABSTRACT**	**c. THIS PAGE**	SAR	24	**19b. TELEPHONE NUMBER** *(include area code)*
Unclassified	**Unclassified**	**Unclassified**			N/A

Standard Form 298 (Rev. 8-98)
Prescribed by ANSI Std. 239.18

ExB Measurements of a 200 W Xenon Hall Thruster

Jared M. Ekholm and William A. Hargus, Jr.

Air Force Research Laboratory, Edwards Air Force Base, CA, 93524

Angularly resolved ion species fractions of Xe^{+1}, Xe^{+2}, and Xe^{+3} in a low power xenon Hall thruster Busek BHT-200 plume were measured using an E×B probe under a variety of thruster operating conditions and background pressures. The thruster was operated at several operating conditions by varying the anode potential of the thruster from 200 V to 325 V in 25 V increments. Measurements of the ion species fractions were made ±90° from thruster centerline 60 cm downstream of the exit plane. At reduced discharge voltages, the species fractions of multiply-charged xenon ions were lower, while at increased discharge voltages, Xe^{+2} and Xe^{+3} showed an increase in their respective ion species fractions. At angles greater than ±35°, a low energy peak was observed suggesting additional collisions in the far-field produce a low energy ion population. Finally, measurements were directed toward characterizing chamber backpressure effects on the plume species fractions at oblique angles between 35-90°. In the presence of additional background neutrals, production of multiply-charged ions increased throughout the plume as a result of increased collisions and scattering.

Nomenclature

$\vec{B}$	magnetic field
B	magnetic field strength [T]
d	distance between plates [m]
$\vec{E}$	electric field
E	electric field strength [V/m]
E_i	ion energy [eV]
e	elementary charge [C]
F	Lorentz force [N]

m_i	ion mass [kg]
q	charge
q_i	charge state of ion
$\vec{u}$	ion velocity [m/s]
v_i	acceleration voltage [V]
V_p	probe voltage [V]
γ_i	secondary electron emission coefficient
ζ_i	ions species fraction

I. Introduction

The Hall effect thruster has been identified as a candidate technology for Earth orbit applications such as station keeping, orbit raising and transfers where propellant mass savings are particularly beneficial. Hall thrusters have achieved high thrust efficiencies approaching 50% through the ionization and acceleration of xenon ions through a main discharge chamber in which the accelerated ions achieve velocities of 15 to 20 km/s at energies in excess of 200 eV. In addition to providing thrust, the highly accelerated ions erode and sputter incident surfaces possibly degrading sensitive spacecraft components such as optics and solar arrays. In light of this, the physics governing the Hall thruster plume must be thoroughly understood, and the energetic ion and spacecraft surface interactions need to be fully characterized. In addition to singly ionized Xenon, Xe^{+1}, multiply-charged species, Xe^{+2} and Xe^{+3}, have been observed in the Hall thruster plume.[1] These multiply-charged high energy ions not only lead to decreased efficiency in the Hall thruster itself, but have a potentially harmful effect on the spacecraft components due to higher erosion and sputtering rates. The production and distribution of these ions were investigated using an E×B probe revealing significant multiply-charged ion populations increasing with angle from centerline. The goal of this work is to characterize the production and distribution of these high energy ions focusing on highly divergent plume angles, $\pm 35^\circ$ from centerline, where interactions with spacecraft surfaces are most likely.

II. Apparatus

A. Function of the E×B Probe

Also known as the Wein Filter, the E×B probe acts as a velocity filter separating ions by their respective masses and charges. Assuming all ions were accelerated through the same potential, ions with differing charge states created within the discharge chamber will

experience similar acceleration potentials resulting in vastly different velocities. As explained by Kim and Hofer,[2,3] the E×B probe separates the charged particles through the use of the Lorentz Force.

$$\vec{F} = qe(\vec{E} + \vec{u} \times \vec{B}) \tag{1}$$

This equation illustrates the force acting on a charged particle moving within electric and magnetic fields. Utilizing this fundamental aspect of nature, one may balance the electric and magnetic fields to achieve a zero net force.

$$0 = qe(\vec{E} + \vec{u} \times \vec{B}) \tag{2}$$

This allows the ions of a particular velocity increment to pass through the typically orthogonal electric and magnetic region undeflected, relating the velocity of the charged particles to the electric and magnetic fields.

$$u = -\frac{\vec{E}}{\vec{B}} \tag{3}$$

Ions which successfully pass through the probe unhindered impacted a conductive collector and were recorded as current. The corresponding probe voltage is then related back to the energy of the ion which successfully traversed the E×B region.[2]

$$E_i = q_i v_i = \frac{m_i}{2e}\left(\frac{V_p}{dB}\right)^2 \tag{4}$$

From the resulting velocity distribution, the ratio of the ion species peaks, ξ_i, is determined, and the relationship between the ion species fractions may be expressed.[3]

$$\Omega_i = \frac{q_i^{\frac{3}{2}}\zeta_i}{\sum_i \left(q_i^{\frac{3}{2}}\zeta_i\right)} \sum \zeta_i = 1 \tag{5}$$

B. Experimental Apparatus

These experiments were conducted in Chamber 6 located at the Air Force Research Laboratory (AFRL) Electric Propulsion Laboratory located at Edwards AFB, CA. Chamber 6 measures 1.8 m diameter and 3.0 m length with a pumping speed of 32,000 l/s on xenon using four single stage cryopanels and one 50 cm dual stage cryopump. During nominal chamber operations chamber pressure is approximately 6×10^{-6} Torr, corrected for xenon. While investigating the effects of increased backpressure, the background pressure was increased to 5×10^{-5} Torr by injecting additional Xe neutrals into the chamber.

The Busek Co, Inc. BHT-200 xenon Hall thruster was used in this experiment. The BHT-200 produces 12 mN of thrust at a system efficiency of 35% while operating at nomi-

nal discharge voltages and conditions, see Table 1. Propellant flow rate was maintained at 940 ug/s with 10% flow to the cathode. During operations the magnet current was maintained at 0.75 A for increased stability due to the presence of plasma oscillations which produced visual fluctuations in the thruster plume. Prior to all measurements, the thruster operated for a minimum of 30 minutes to ensure thermal equilibrium within the thruster as well as background pressure stabilization.

Figure 1 depicts the E×B probe identifying the orientation of the electric and magnetic fields with respect to the direction of the collimated ionic beam. As ions with velocity, $\vec{u}$, enter the test section, they are deflected by the Lorentz force, as seen by the path of the deflected ion, unless traveling at the desired velocity as determined by Eqn. 3. The E×B probe consists of three main sections: the entrance collimator, E×B filter section, and exit collimator. The entrance collimator measures 88 mm in length with an entrance cap orifice of 1.6 mm. This section allows a narrow beam of charged particles to enter the E×B filter region. The E×B filter section measures 152.0 mm in length with apertures of 1.6 mm at each end. As particles enter the E×B filter section, they are subjected to an electric field generated by two parallel bias plates and an orthogonal magnetic field produced by two permanent magnets. The voltage between the two bias plates was swept from 0 to 60 V in 0.2 V increments, one plate ramped positive and the other negative with respect to ground using an Aglient 6614C precision voltage supply. Two 1 MΩ resistors were used to ensure a symmetric potential was created between the two plates. The average magnetic field strength of 0.129 T and a peak flux of 0.163 T was measured at the center of the E×B region. For the purpose of analysis, the value of B in Eqn. (4) is taken to be the geometrical mean of the magnetic field through the entire E×B test section. With the magnitude of the magnetic field set at 0.129 T sweeping the current from 0 to 60 V is sufficient to deflect all ions with energy less than 1500 eV. To minimize the build up of pressure within the E×B test section, several 0.25 inch holes were bored in the rear plate. These holes improved throughput preventing the formation of a localized high pressure zone within the E×B region, decreasing the likelihood of further collisions occurring within the probe itself. Ions which transverse the E×B section unhindered exit through the output collimator impacting a tungsten coated ion collector and measured as current. The exit collimator measures 140 mm in length terminating at the tungsten coated cupped ion collector. The cupped cylindrical geometry of the ion collector captures all secondary election emissions as a result of ion impingement. The resultant current was measured on a Kiethley 6485 picoammeter, capable of measuring currents as low as 20 fA. All instruments, including the thruster and probe, were referenced to chamber ground.

The thruster was mounted on a rotation stage so ion species could be measured at various angles off thruster centerline. The rotational axis was aligned with center of the thruster

face plate ensuring constant axial distance was maintained from the probe through all angles. The probe was fixed to a stationary pedestal 60 cm from the thruster and laser aligned with the nose cone. The dimensions of the vacuum chamber allowed investigations up to ±90° from the thruster's vertical centerline.

Due to the geometry of the E×B probe, special attention was given to alignment with the thruster. The acceptance angle to the nose cone of the thruster was limited to ±0.5° and a distance of ±1 cm from the thruster nose cone. Preliminary calculations into the uncertainty of the probe were performed as described by Kim.[2] Based on the dimensions and acceptance angles of both the entrance and exit collimator, the probe has a minimum calculated uncertainty of ±4 eV. Fringing effects of both the magnetic and electric fields as well as the ram effect were not taken into consideration in calculating this uncertainty. These factors will only increase the actual uncertainty of the probe.

III. Results and Analysis

A. Calibrations and Testing

Initial investigations in the plume showed the E×B probe capable of distinguishing the respective Xe ion species. At each of the operating conditions, the voltage applied to the bias plates swept from 0 to 60 V while the collector current was recorded. A range of 60 V proved sufficient to clearly distinguish the various Xe signals as predicted and illustrated in Fig. 2. Although a fourth peak, Xe^{+4}, was occasionally detected, its very low magnitude produced negligible effects on the species fractions and will not be addressed further. Signal broadening and over-lapping between the peaks was recorded, possibly due to collisions in the plume but also within the E×B probe itself. Broadening is more apparent in the multiply-charged species than Xe^{+1}, suggesting the multiply-charged ions are created further downstream and at higher angles from the thruster exit plane as seen by King.[4] This phenomena described in detail by Beal[5] attributes several factors explaining the presence of multiply-charged ions within the wings of the plume to include discharge chamber geometry and a secondary ionization region. Also seen in Fig. 2, a small amount of overlapping occurs between each respective peak. This increases with angle from thruster centerline possibly due to elastic collisions as explained by Kim.[2]

Signal broadening in Fig. 2 becomes apparent as Xe^{+3} has a measured full width at half maximum (FWHM) of 40 eV whereas Xe^{+1} has a FWHM of 20 eV. In addition, signal overlap between Xe^{+2} and Xe^{+3} raises concerns of glancing collisions between species within the plume as well as differentiation of the various species. These initial data also served to calibrate the probe. While operating at 250 V, the Xe^{+1} peak was recorded at 173.0 eV, corresponding to a velocity of 16,000 ± 500 m/s. This is in agreement with published values

of Hargus and Charles' LIF, laser induced fluorescence, measurements of the same thruster.[6] From the LIF data, Xe^{+1} had a velocity of 16,300 ± 500 m/s, well within the uncertainty. In addition to the uncertainty calculated through Kim's method, additional comparisons were made using the LIF data. Through these comparisons, it is assumed the E×B probe has a velocity measurement uncertainty of approximately ±8%.

Baseline stability issues occurred in earlier work prompting an investigation to find a resolution. The ram effect possibly explains the observed variable baselines and is a concern with the data quality. With the probe oriented directly at the thruster, ions from the plume are trapped within the probe creating a localized high pressure volume. Upon rotating the thruster to a new measurement position, a 10 minute pressure stabilization delay appeared to equalize conditions within the probe. The procedure proved adequate in subsequent tests and greatly diminished baseline variations. This delay was performed prior to each measurement due to decreasing ion flux through the probe at increasing angles. In addition, 10 voltage sweeps of each angle were recorded and averaged, creating a smooth data set. The net effect of this procedure is to increase the signal to noise ratio by approximately 3×.

B. Angles Greater than 35°

Ion behavior at highly divergent angles is of particular interest because charge-exchange and spacecraft interactions are most likely to occur in this region of the plume. Specifically the distribution of multiply-charged ions requires a thorough analysis due to their high kinetic energies and erosion rates on spacecraft surfaces. For these reasons, the ion species fractions at oblique angles were also mapped.

At large angles, plume interaction with the chamber wall occurred. Although the measurements up to ±90° are achievable, measurements beyond ±80° were unusable due to a combination of instrumental uncertainty, decreased signal strength and low signal to noise ratios (SNR) and consequently omitted from this paper. Data recorded at these angles was obscured by noise making the peaks indistinguishable from the background noise.

Current traces, recorded under nominal thruster operating conditions, are seen in Fig. 3 for wide plume angles. Distinct peaks corresponding to Xe^{+1}, Xe^{+2}, and Xe^{+3} are clearly visible at expected velocities and energy levels. Xe^{+3} is obscured by background noise and no longer distinguishable beyond 70°. As expected, signal strength lessens as a function of angle corresponding to a reduction in ion flux.

The ion species fractions were first investigated to determine the distribution of multiply-charged ions throughout the thruster plume. The ion species fractions were calculated using the signal peak heights described by Hofer, Gallimore, and Kim.[2,3,7] Figure 4 depicts the resulting distribution of the ions within the plume and corresponding species fractions. Multiply-charged ion fractions increase with plume angle which has also been shown by Beal.[5]

In addition, Xe^{+1}, which dominates the plume, decreases from 0.991 to 0.853 between 35° to 80°. Of particular interest, the region approximately 45±10°, Xe^{+1} experiences a sharp decrease within the plume while the population fraction of multiply-charged ions increases as seen in Fig. 4. As seen in Fig. 4, the formation of an extra peak at roughly 90 eV was unanticipated. Its occurrence prompted analysis to characterize this unidentified peak and to determine its origin.

C. Effect of Anode Potential Variance on Ion Species Fractions

To uncover the effects of anode potential on ion species fraction distribution, the thruster anode potential was varied from 200 V to 325 V in 25 V increments. As expected, Fig. 5 shows a shift toward higher energy for all three ion species corresponding to increasing anode potential.

Table 2 shows a comparison of the species fractions as the anode potential is varied; all other parameters were maintained at nominal conditions while the E×B probe was oriented along thruster centerline. The results indicate an increase in Xe^{+2} and Xe^{+3} at off-nominal operating potentials with a resulting decrease in Xe^{+1} species fraction. The data clearly show ion species fractions and multiply-charged ion production is linked to anode potential.

At the nominal 250 V anode potential, singly ionized xenon species fraction achieves a maximum fraction of 0.955, whereas the doubly and triply charged xenon achieve species fractions of 0.038 and 0.007 at the centerline. Figure 5 depicts the ion species fractions of each Xe^{+1}, Xe^{+2}, and Xe^{+3} at the respective anode potential. Xe^{+1} dominates in all cases, yet at an elevated operating anode potential of 325 V, multiply-charged ions compose nearly 10% of the ion flux. As the anode potential increases to the optimal conditions, Xe^{+1} production steadily increases as Xe^{+2} and Xe^{+3} production declines. It is interesting to note at 250V, the nominal operating condition for the BHT-200, Xe^{+1} achieves a local maxima whereas Xe^{+2} and Xe^{+3} production is at a minimum.

IV. Effects of Chamber Backpressure

An increase in background pressure within the vacuum chamber increases the possibility of ion-neutral collisions within the plume, as well as producing additional ion flux due to neutral ingestion. With additional collisions, an increase in multiply-charged ion production as well as a corresponding decrease in singly-charged ions is expected. For this reason, ion behavior at oblique angles was investigated at an elevated background pressure. Additional xenon gas was introduced into the chamber increasing the background pressure to 5×10^{-5} Torr, an 8× increase in background pressure.

As seen in Fig. 6, the increased background pressure data share many characteristics

with the traces measured at lower background pressures. The measured energy of Xe^{+1} and Xe^{+2} were identical, while Xe^{+3} could not be distinguished from these traces at angles greater than 60°. Along thruster centerline, direct comparison between the two background pressures revealed little change in peak signal strength. In addition several differences were noted between the two background pressures. Figure 6 clearly shows the appearance of the unidentified peak at 90 eV at 80° whereas at nominal background pressures the peak appeared at 50°. In addition, the measured signal increased by nearly a factor of 10 but also increased signal noise with elevated chamber backpressure.

At nominal pressures, signal broadening introduces uncertainties in calculating the ion species fractions. Since the peak height is used in this effort to determine species fractions, a peak with relatively low signal strength but spread across a wide range of energies will not be accurately weighed against other peaks. For this reason the effects of signal broadening must be acknowledged during analysis. With elevated chamber backpressure, signal broadening did not increase at angles less than 60°. Yet at angles greater than 70°, the increased backpressure produced a significantly wider energy distribution. The effects introduced by signal broadening were not quantitatively measured during this investigation, but it can be assumed this broadening introduces additional uncertainty into the ion species measurements at oblique angles.

Elevated background pressure ion species fractions mirrored that at nominal background pressure as seen in Fig. 7. Xe^{+1} fraction decreased as a function of angle with a maximum of 0.943 at 5° and minimum of 0.736 at 80°. Unlike Fig. 4, the ion species fractions did not experience a substantial decrease at 45°, but instead all species fractions leveled. Beyond 45°, multiply-charged ion fractions continued to increase as singly-charged ion production decreased at substantially lower rates. Table 3 clearly shows the difference between the ion species fractions between the nominal and high background pressure test cases. Xe^{+1} fraction decreased as a function of pressure while Xe^{+2} and Xe^{+3} fraction increased by a factor of 2.5.

After characterization of the ion species fractions at elevated chamber pressures, possible physical explanations can be made to explain multiply-charged ion fraction trends. As noted before, the elevated chamber backpressure corresponds to an increase in ion-neutral collision events. It is possible the increased populations of multiply-charged ions are a result of Xe neutral back-flow into the ionization region. The increased population of neutrals within the ionization region yield greater opportunity for ion-neutral collisions corresponding to an increase in multiply-charged ions. This appears to be a very likely scenario since the only multiply-charged ions this study can clearly identify are those which are accelerated through the same potential as Xe^{+1}.

V. Characterization of Unidentified Peak

As seen in Fig. 6, an unidentified peak appears before the Xe^{+1} peak at 90 eV. This unexpected peak is also seen by King during his analysis of the oblique angles using a parallel plate energy analyzer.[4] King relates these peaks to charge-exchange collisions within the plume. However, the energy associated with these ions (65 through 90 eV) is somewhat higher than expected for a charge-exchange collision.

Figure 8 depicts the emergence of the unidentified peak from the Xe^{+1} peak. The unidentified feature is first visible at 35° but is not fully distinguishable from Xe^{+1}. As the measurement angle increases, the feature becomes more distinct eventually forming a separate easily identifiable peak at 45°. In addition, the appearance of significant signal overlapping between Xe^{+1} and Xe^{+2} suggests possible collisions between the two ion species. A detailed discussion of both inelastic and elastic plume collisions between various ion species and background neutrals can be found in E×B investigations by both King and Kim.[4,2] In its simpliest explanation, elastic collisions between Xe^{+1} and Xe^{+2} will result in an ion population with energies between each of the respective species. Since momentum is conserved, the resulting ions will have a velocity slightly higher or lower depending on the original charge state. These collisions will appear as a distinct ion population with an energy distribution between the peaks of the original ion species as seen in Fig. 8.

In order to characterize the unidentified feature, the peak's signal strength in relation to Xe^{+1} were mapped in Fig. 9. As expected, the signal strength of the unidentified peak decreases with increasing angle due to reduced ion flux at the wide divergent angles of the plume. Also seen was a substantial drop in signal strength at 45°, the same angle in which the peak became distinguishable from Xe^{+1} and multiply-charged ion production substantially increases as shown in Fig. 4.

The peak signal strength of Xe^{+1} and the unidentified peak were also compared as seen in Fig. 9 between 0° and 80° from thruster centerline at both nominal and elevated background pressures. At angles near 35°, where the unidentified feature is distinguished from Xe^{+1}, the signal strength of Xe^{+1} is approximately an order of magnitude greater than the unidentified feature. Although the unidentified feature has a maximum energy of 2.5 nA at 35°, the Xe^{+1} signal dominates with a peak signal intensity of 11.6 nA. However as the angles increase beyond 35°, the signal strength of Xe^{+1} declines sharply until both Xe^{+1} and the unidentified peak attain comparable signal intensities of 0.5 nA at 50°. Beyond 50°, both peaks maintain similar signal strengths with little deviation. At elevated backpressures both the Xe^{+1} and the unidentified peak shared common characteristics. Appearing at 60° the unidentified feature's signal strength was measured at 5 nA similar to Xe^{+1}. The signal strength of both peaks steadily decline at similar rates to 1.75 nA at 80°. Also of interest,

Fig. 9 shows the sizable differences in overall signal strength between nominal and elevated background pressures. At 80° and under elevated backpressure conditions, the lowest measured signal strength of 1.75 nA was greater than measured signal strength at 45° under nominal conditions indicating ion flux at elevated backpressures is roughly double that of nominal backpressures at oblique angles.

The formation of the unidentified peak under elevated chamber pressure can be seen emerging from the Xe^{+1} peak in Fig. 6. With increased backpressure, the unidentified peak signal increased by only 5x whereas the peak signal strength increased 10× under nominal pressures as seen in the Xe^{+1} ion peaks in Fig. 3.

VI. Conclusions

The ion species fractions of a BHT-200 vary considerably throughout the plume. Anode potential, angle from centerline, and chamber backpressure clearly have an effect on the species fractions and distribution of multiply-charged ions.

At highly divergent angles, ion species fractions show strong dependence on angle. As expected, signal strength decreases as ion flux at wide angles is greatly reduced. For this reason, special measures were required to reduce noise and enhance the signal strength at these angles. Xe^{+1} dominates at angles less than 45°, but beyond 45°, Xe^{+1} fractions decline due to increasing fractions of multiply-charged ions. At 35° a separate, yet unidentified, peak emerges from the Xe^{+1} signal eventually becoming a distinct peak growing as a function of the angle. Although significant overlapping occurs, the unidentified peak distinguishes itself from the other species at angles greater than 45°. Eventually, the peak attains a signal strength comparable to Xe^{+1}. Several possible explanations as to the origin of this unidentified feature including elastic and charge-exchange collisions are possible, yet its identification and origin remain unclear.

Anode potential directly affects the fractions of all three ion species. Measurements indicate the Xe^{+1} species fraction is 0.955 at the nominal operating condition, 250 V, and then falls to 0.913 at an anode potential of 200 V. Whereas the multiply-charged ions, Xe^{+2} and Xe^{+3}, species fractions remain lowest at the nominal operating condition and higher elsewhere.

Chamber backpressure and greater plume angle increased multiply-charged ion production. Yet as signal increased, noise also became an issue. In comparison to nominal operating pressures, increased backpressure within the chamber yielded higher Xe^{+2} and Xe^{+3} ion species fractions although Xe^{+1} continued to dominate the plume. At nominal vacuum chamber backpressures, the unidentified feature appeared at 45° possibly due to collisions within the probe resulting in signal broadening or reduced SNR. In addition, the appearance

of the additional peak at 90 eV did not distinguish itself until 70°.

VII. Acknowledgments

The authors thank Richard Hofer from NASA Glenn Research Center for supplying the mechanical drawings for the E×B probe as well as Garrett Reed and Michael Nakles of AFRL, and David Scharfe of Stanford University for assistance with the data acquisition software and initial stages of this effort.

References

[1]Manzella, D. H., "Stationary Plasma Trurster Plume Emissions," *International Electric Propulsion Conference*, 1993, IEPC-93-097.

[2]Kim, S. W., *Experimental Investigations of Plasna Parameters and Species-Dependent Ion Energy Distribution in the Plasma Exhaust Plume of a Hall Thruster*, Ph.D. thesis, University of Michigan, Ann Arbor, MI, 1999.

[3]Hofer, R. R. and Gallimore, A. D., "Ion Species Fractions in the Far-Field Plume of a High-Specific Impulse Hall Thruster," *39th Joint Propulsion Conference*, Huntsville, AL, 2003, AIAA-2003-4556.

[4]King, L. B., *Transport-Property and Mass Spectral Measurements in teh Plasna Exhaust Plume of a Hall-Effect Space Propulsion System*, Ph.D. thesis, University of Michigan, Ann Arbor, MI, 1998.

[5]Beal, B., *Clustering of Hall Effect Thrusters For High-Power Electric Propulsion Applications*, Ph.D. thesis, University of Michigan, Ann Arbor, MI, 2003.

[6]Hargus Jr., W. and Charles, C. S., "Near Exit Plan Velocity Field of a 200W Hall Thruster," *39th Joint Propulsion Conference*, Huntsville, AL, 27-29 July 2003.

[7]Kim, S. W. and Gallimore, A. D., "Plume Study of a 1.35 kW SPT-100 using an ExB Probe," *35th Joint Propulsion Conference*, Los Angeles, CA, 1999, AIAA-99-2423.

Table 1. Nominal Operating Conditions: ***Typical operating conditions of the Busek BHT-200 Hall thruster.***

Anode Flow	840 μg/s (Xe)
Cathode Flow	98 μg/s (Xe)
Anode Potential	250 V
Anode Current	0.85 A
Heater Current	3.0 A
Keeper Current	0.5 A
Magnet Current	0.75 A

Table 2. Ion Species Fractions of the BHT-200 Measured at the Centerline (60cm): *Maximum singly-charged ion production at nominal conditions.*

Anode (V)	Xe^{+1}	Xe^{+2}	Xe^{+3}
200	0.913	0.066	0.021
225	0.937	0.050	0.013
250	0.955	0.037	0.008
275	0.953	0.040	0.008
300	0.950	0.042	0.008
325	0.939	0.050	0.011

Table 3. Ion Species Fractions of the BHT-200 at Elevated Backpressure. ***Comparison of nominal pressure vs. high pressure and effects on ion species fractions.***

Xenon Ion Species Fractions Nominal / Elevated Backpressure			
Deg	Xe^{+1}	Xe^{+2}	Xe^{+3}
0	0.991 / 0.937	0.008 / 0.049	0.0006 / 0.013
20	0.989 / 0.864	0.010 / 0.100	0.001 / 0.032
40	0.968 / 0.766	0.030 / 0.168	0.002 / 0.067
60	0.939 / 0.748	0.053 / 0.176	0.008 / 0.075
80	0.853 / 0.736	0.111 / 0.184	0.035 / 0.080

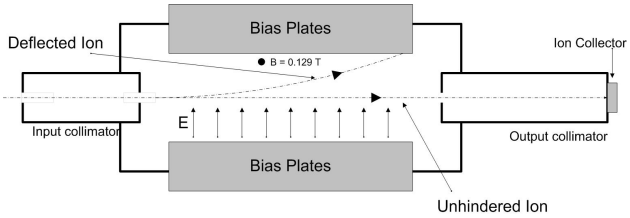

Figure 1. Electric and Magnetic Fields within the E×B Probe. ***Path of unhindered and deflected ions transversing the E×B section.***

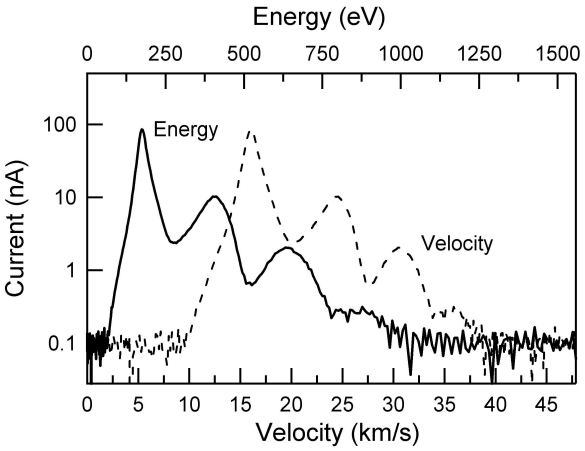

Figure 2. Energy and velocity trace of 250 V ion species fractions: E×B Probe. ***Note the*** Xe^{+1} ***signal intensity and detail.***

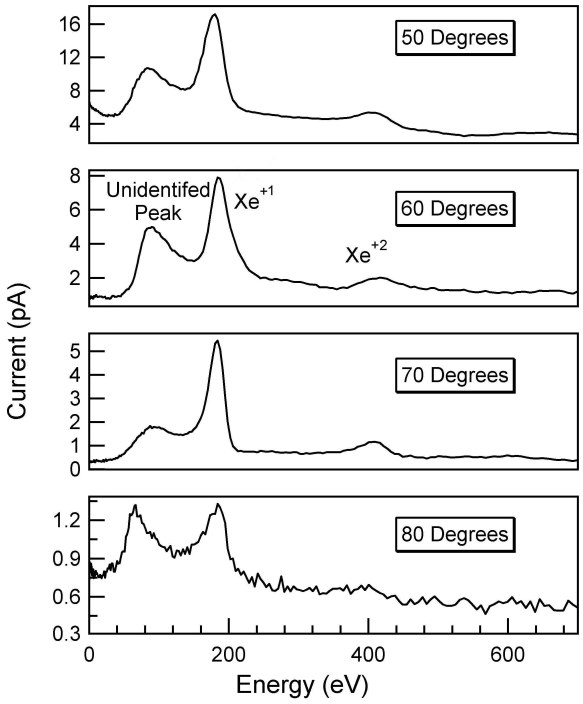

Figure 3. Energy Distribution at 50°, 60°, 70° and 80°. ***Note the appearance of an unidentified peak at ≈90 V.***

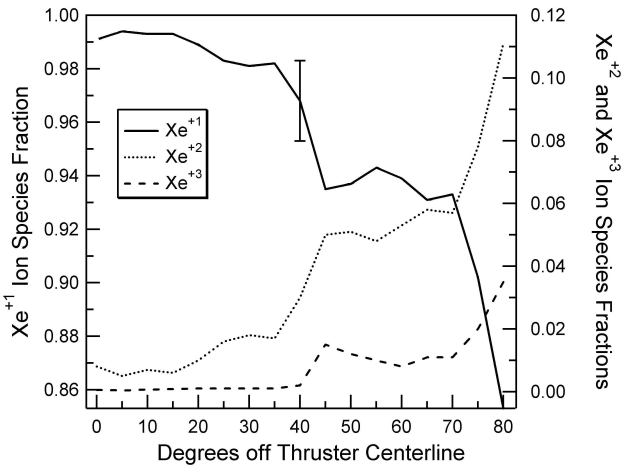

Figure 4. Ion Species Fractions in the Far-Field ***Note the decrease of*** Xe^{+1} ***and the corresponding increase of multiply-charged ions emphasized at 45°. All measurements were taken at 5° increments.***

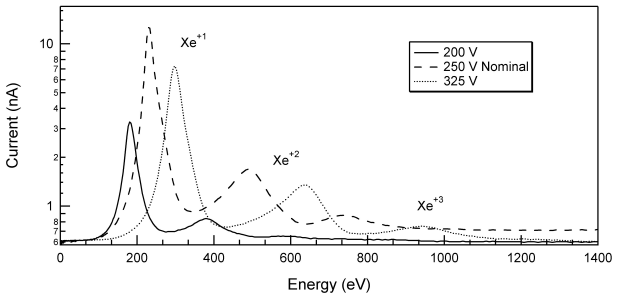

Figure 5. 200-325 V Effects on Ion Species Fractions ***Note the increase in energy as a function of increasing anode potential along thruster centerline.***

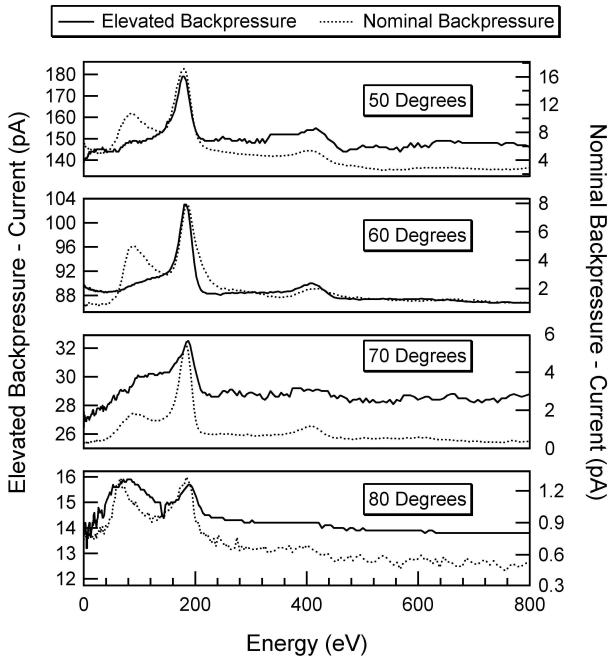

Figure 6. Energy Distribution at 50°, 60°, 70° and 80°. ***Note the comparison to nominal backpressure traces.***

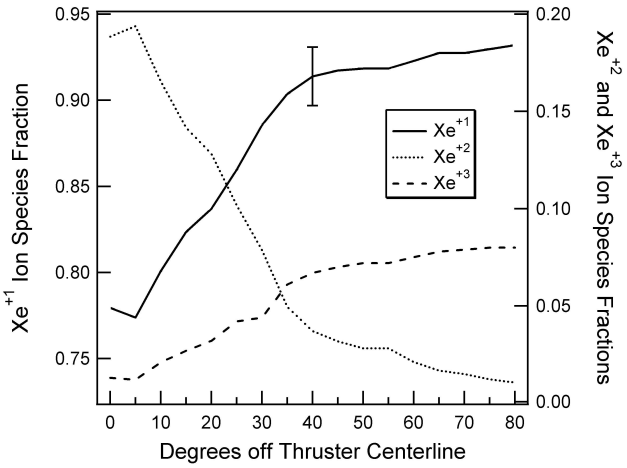

Figure 7. Ion Species Fractions at Highly Divergent Plume Angles. ***Note leveling effect beyone 45° illustrating effect of backpressure on plume divergence and charge-exchange production.***

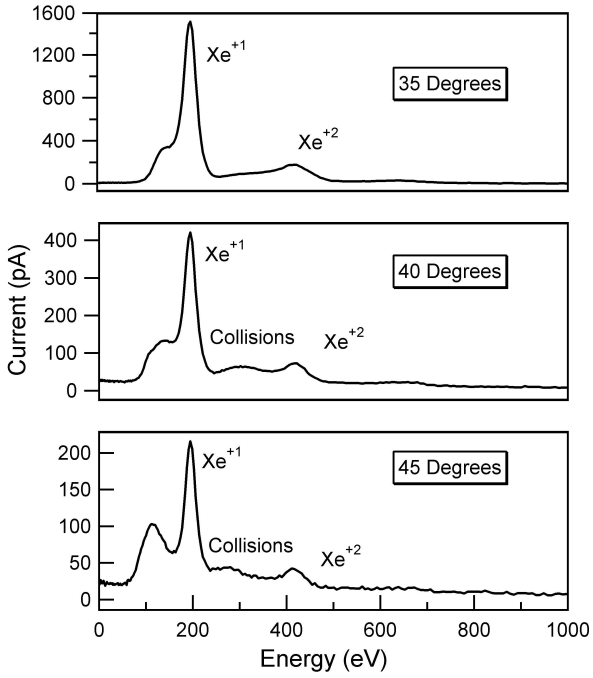

Figure 8. Emergence of Unidentified Peak: ***As angle increases the unidentified peak becomes distinct from the*** Xe^{+1} ***peak.***

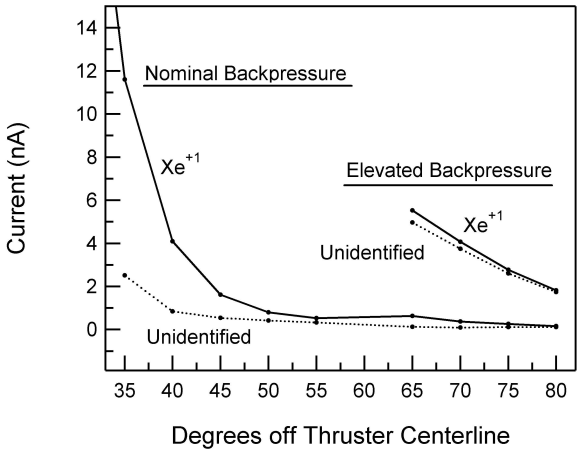

Figure 9. Xe^{+1} and Unidentifed Peak Intensity Comparison: ***Comparable intensities at 45°. Also note relationship at elevated backpressure.***